# Structure Dynamic Analysis of C-9 Parachute Using Absolute Nodal Coordinate Formulation Thin Shell Element

Fan Liu, Ying Tong*, Lu Zhang, Yongfei Mo

China Aerodynamic Research and Development Center, Mianyang, Sichuan, 621000, China

*Corresponding author's e-mail: lshtongying@163.com

**Abstract.** In parachute fluid structure interaction (FSI) simulation, traditional parachute structure discrete methods including classic finite element method and mass-spring-damp method suffers from its large computational cost and deficiency in describing material property. This paper develops a generic shell element based on absolute nodal coordinate formulation (ANCF) to model parachute canopy to reduce computation resources and retain membrane strain/stress analyzing capability. We conduct multiple validation cases of ANCF plate and shell element and compare with current literature, in which large deformation configuration and stress distribution have been verified. A 1/4 C-9 parachute canopy inflation process by uniform pressure is simulated by discretizing into 7 ANCF shell and 84 shell element, for which the number of element discretization reduces to 1/10 than classic FEM and computational cost is considerably reduced using band sparse matrix solving technique.

**Keywords:** Parachute, fluid structure, finite element.

## 1. Introduction

As the most significant aerodynamic decelerating equipment, the parachute has been widely applied in aeronautics and astronautics. Typical application scenarios include air drop of personnel and materials, re-entry of manned spacecraft, internally carried rocket air-launch, UAV recovery. In order to satisfy the requirements of decelerate efficiency, safety and digitalization; it is necessary to improve the design, evaluation and optimization of parachute system.

Structure dynamics is particularly critical to solve parachute mechanical problems. During inflation and descent period, the canopy of parachute exhibits large deformation under unsteady aerodynamic load. The mechanism of parachute deformation and movement involve elastic mechanics, multiple body dynamics, and flight dynamics. Numerical simulation of parachute based on pure theoretical model shows significant advantage over flight test and wind tunnel experiment in cost and evaluation response speed. This methodology also cancels the empirical parameter and provides high fidelity structure modeling.

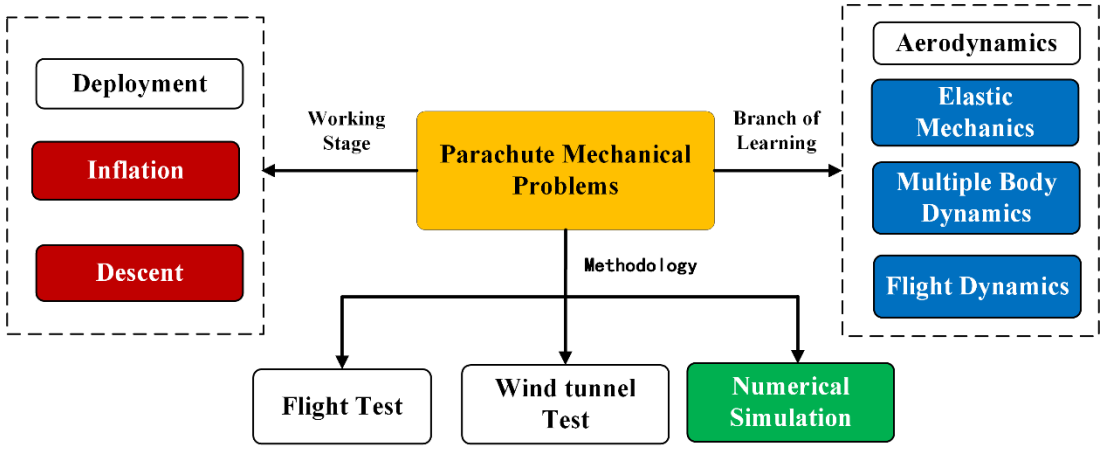


**Figure 1.** Structure dynamics simulation in parachute mechanical

With the rapid development of computational structure dynamics (CSD) in recent 40 years, the main numerical techniques used in parachute simulation include the mass-spring-damper (MSD) method and finite element method (FEM).

MSD method was first presented by Purvis[3-4] in the 70s and 80s to solve parachute FSI. Miyoshi[5] and Li[6-7] upgraded MSD by considering fabric tensile stiffness and angular stiffness. However, the deficiency in modeling continuous surface remains makes it highly difficult in handling non-linear material constitutive property by MSD.

Tezduyar[8-9] has been working in solving parachute structure and fluid dynamics both in FEM method. Karagiozis[10] et al. model supersonic parachute with $C^1$-conforming subdivision membrane finite element. As classical FEM is based on small deformation/strain assumption, a large scale of discretization mesh ($10^3$~$10^4$ elements) is needed (Fig. 2 and Fig.3) to model large deformation and non-linear strain of parachute canopy and thus causes vast computation demand.

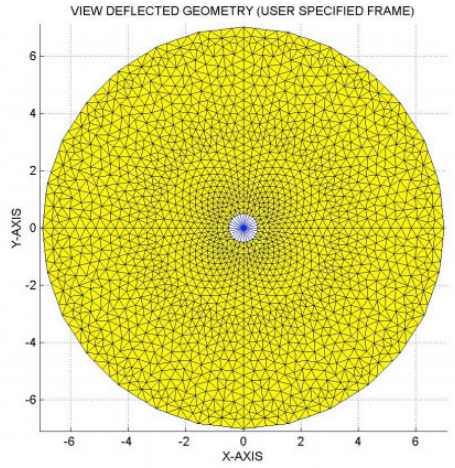


**Figure 2.** Cut pattern of C-9 parachute canopy [1] discretized with 3584 triangle membrane elements

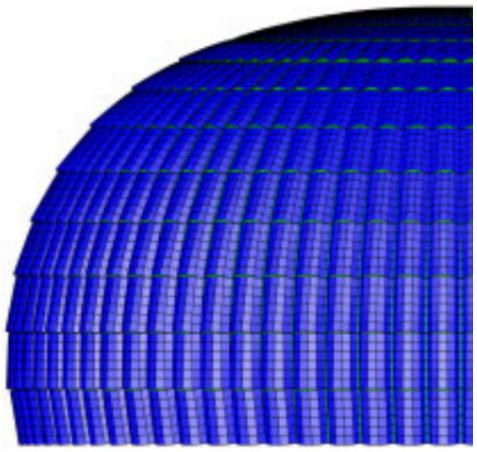

**Figure 3.** Canopy structure mesh [2] discretized with 26000 four-node quadrilateral membrane elements

A modern structure dynamics approach that can both describe material/geometrical nonlinearities and avoid large-scale parallel computation is urgently need. This paper presents the idea of introducing absolute nodal coordinate formulation (ANCF) in parachute structure simulation. Shabana[11] first proposed ANCF as a nonlinear finite element theory. The nodal coordinates in ANCF are chosen to be the global spatial coordinates and gradients, while the classical FEM uses local incremental displacements/rotations[12-13]. An ANCF can be use to obtain a simple description of rigid rotations for flexible bodies and to reduce nonlinearities in solving the dynamics equations. Since it is based on a high-order FEM, the application of the classical FEM to discretize the same elastic structure at a much smaller mesh scale results in a much lower computational cost[14-17].

## 2. Theory of generic ANCF thin shell structure dynamics

The ANCF thin plate elements are based on degenerate three-dimensional continuum shell behavior. In this case, the shells are defined by their mid-surfaces by assuming that the fibers straight and normal to the mid-surface remain straight during the deformation.Moreover, we assume the stress normal to the shell mid-surfaces is zero throughout the shell motion.

In the absolute nodal coordinate formulation, the global position vector of an arbitrary point on afinite element is defined in the inertial frame using the following equation:

$$\boldsymbol{r} = \boldsymbol{S}\left(x, y, z\right)\boldsymbol{e}_0$$

where $\boldsymbol{r}$ is the global position vector of an arbitrary point $P$ on the plate; $x$, $y$ and $z$ are the spatial coordinates of the plate defined in the element coordinate system; $\boldsymbol{S}$ is the element shape function matrix. As in Fig.4, $\boldsymbol{e}$ is the vector of nodal coordinates:

$$\boldsymbol{e}=\begin{bmatrix}\boldsymbol{e}_1 & \boldsymbol{e}_2 & \boldsymbol{e}_3 & \boldsymbol{e}_4\end{bmatrix}^T \text{ where } \boldsymbol{e}_i=\begin{bmatrix}\boldsymbol{r}_i & \frac{\partial \boldsymbol{r}_i}{\partial x} & \frac{\partial \boldsymbol{r}_i}{\partial y} & \frac{\partial \boldsymbol{r}_i}{\partial z}\end{bmatrix}^T \quad i=1,2,3,4$$

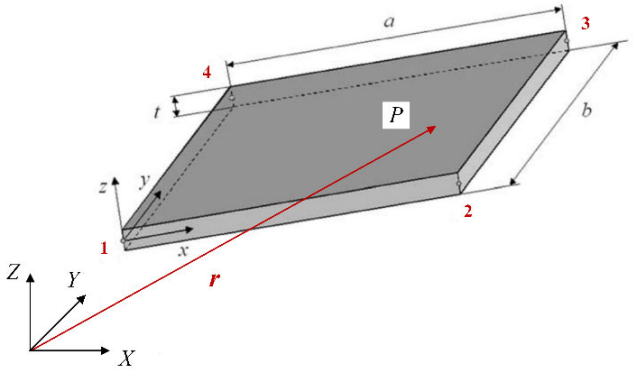


**Figure 4.** Four node ANCF plate/shell element

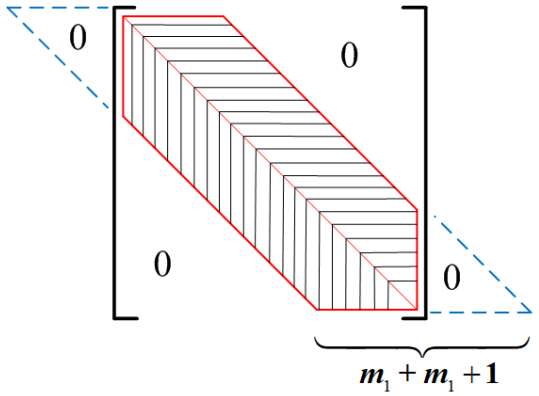


**Figure 5.** Band sparse matrix reshaping

In order to obtain a generalization of the preceding formulation to shell elements, a mapping between simple geometries in a local coordinate system [$x$ $y$ $z$] and surfaces in a global Cartesian coordinate system [$X$ $Y$ $Z$] is needed. The global displacement gradient Jacobi matrix is

$$\boldsymbol{J}=\frac{\partial \boldsymbol{r}}{\partial \boldsymbol{X}}=\begin{bmatrix}\boldsymbol{r}_X & \boldsymbol{r}_Y & \boldsymbol{r}_Z\end{bmatrix}=\begin{bmatrix}\frac{\partial r_1}{\partial X} & \frac{\partial r_1}{\partial Y} & \frac{\partial r_1}{\partial Z}\\ \frac{\partial r_2}{\partial X} & \frac{\partial r_2}{\partial Y} & \frac{\partial r_2}{\partial Z}\\ \frac{\partial r_3}{\partial X} & \frac{\partial r_3}{\partial Y} & \frac{\partial r_3}{\partial Z}\end{bmatrix}=\begin{bmatrix}\frac{\partial \boldsymbol{S}_1}{\partial X}\boldsymbol{e} & \frac{\partial \boldsymbol{S}_1}{\partial Y}\boldsymbol{e} & \frac{\partial \boldsymbol{S}_1}{\partial Z}\boldsymbol{e}\\ \frac{\partial \boldsymbol{S}_2}{\partial X}\boldsymbol{e} & \frac{\partial \boldsymbol{S}_2}{\partial Y}\boldsymbol{e} & \frac{\partial \boldsymbol{S}_2}{\partial Z}\boldsymbol{e}\\ \frac{\partial \boldsymbol{S}_3}{\partial X}\boldsymbol{e} & \frac{\partial \boldsymbol{S}_3}{\partial Y}\boldsymbol{e} & \frac{\partial \boldsymbol{S}_3}{\partial Z}\boldsymbol{e}\end{bmatrix}$$

in which $\boldsymbol{S}_i$ is the $i$th row of shape function $\boldsymbol{S}$. Using the chain rule of partial differentiation, one obtains

$$\begin{bmatrix}\frac{\partial S_i}{\partial x}\\ \frac{\partial S_i}{\partial y}\\ \frac{\partial S_i}{\partial z}\end{bmatrix}=\begin{bmatrix}\frac{\partial X}{\partial x} & \frac{\partial Y}{\partial x} & \frac{\partial Z}{\partial x}\\ \frac{\partial X}{\partial y} & \frac{\partial Y}{\partial y} & \frac{\partial Z}{\partial y}\\ \frac{\partial X}{\partial z} & \frac{\partial Y}{\partial z} & \frac{\partial Z}{\partial z}\end{bmatrix}\cdot\begin{bmatrix}\frac{\partial S_i}{\partial X}\\ \frac{\partial S_i}{\partial Y}\\ \frac{\partial S_i}{\partial Z}\end{bmatrix}=\boldsymbol{D}\cdot\begin{bmatrix}\frac{\partial S_i}{\partial X}\\ \frac{\partial S_i}{\partial Y}\\ \frac{\partial S_i}{\partial Z}\end{bmatrix} \qquad i=1,2,3$$

where $\boldsymbol{D}$ is a 3×3 constant matrix defined by shell initial configuration, which is the transformation matrix between partial derivative of local coordinate system and global Cartesian coordinate system.

The shell kinetic energy T and mass matrix is

$$T=\frac{1}{2}\dot{\boldsymbol{e}}^T\boldsymbol{M}\dot{\boldsymbol{e}} \qquad \boldsymbol{M}=\int_V \rho\boldsymbol{S}^T\boldsymbol{S}|\boldsymbol{D}|dV$$

The elastic force of shell element is

$$\boldsymbol{Q}_k=\int_V\left(\frac{\partial \boldsymbol{\varepsilon}}{\partial \boldsymbol{e}}\right)^T\boldsymbol{E}\boldsymbol{\varepsilon}|\boldsymbol{D}|dV$$

where $\boldsymbol{E}$ is the matrix of elastic coefficient, the matrix element of symmetric strain tensor $\boldsymbol{\varepsilon}$ is

$$\varepsilon_{11}=\frac{1}{2}\left(\boldsymbol{r}_X^T\boldsymbol{r}_X-1\right)=\frac{1}{2}\left(\boldsymbol{\alpha}_1^T\boldsymbol{r}_x^T\boldsymbol{r}_x\boldsymbol{\alpha}_1-1\right)\qquad \varepsilon_{12}=\boldsymbol{r}_X^T\boldsymbol{r}_Y=\boldsymbol{\alpha}_1^T\boldsymbol{r}_x^T\boldsymbol{r}_x\boldsymbol{\alpha}_2$$

$$\varepsilon_{22}=\frac{1}{2}\left(\boldsymbol{r}_Y^T\boldsymbol{r}_Y-1\right)=\frac{1}{2}\left(\boldsymbol{\alpha}_2^T\boldsymbol{r}_x^T\boldsymbol{r}_x\boldsymbol{\alpha}_2-1\right)\qquad \varepsilon_{13}=\boldsymbol{r}_X^T\boldsymbol{r}_Z=\boldsymbol{\alpha}_1^T\boldsymbol{r}_x^T\boldsymbol{r}_x\boldsymbol{\alpha}_3$$

$$\varepsilon_{33}=\frac{1}{2}\left(\boldsymbol{r}_Z^T\boldsymbol{r}_Z-1\right)=\frac{1}{2}\left(\boldsymbol{\alpha}_3^T\boldsymbol{r}_x^T\boldsymbol{r}_x\boldsymbol{\alpha}_3-1\right)\qquad \varepsilon_{23}=\boldsymbol{r}_Y^T\boldsymbol{r}_Z=\boldsymbol{\alpha}_2^T\boldsymbol{r}_x^T\boldsymbol{r}_x\boldsymbol{\alpha}_3$$

$$\boldsymbol{\alpha}_1=\begin{pmatrix}a_{11} & a_{21} & a_{31}\end{pmatrix}^T$$
$$\boldsymbol{\alpha}_2=\begin{pmatrix}a_{12} & a_{22} & a_{32}\end{pmatrix}^T\qquad \boldsymbol{D}^{-1}=\begin{bmatrix}a_{11} & a_{21} & a_{31}\\ a_{12} & a_{22} & a_{32}\\ a_{13} & a_{23} & a_{33}\end{bmatrix}$$
$$\boldsymbol{\alpha}_3=\begin{pmatrix}a_{13} & a_{23} & a_{33}\end{pmatrix}^T$$

The generalized load on ANCF shell is defined as

$$\boldsymbol{Q}_e=\frac{\delta W_e}{\delta \boldsymbol{e}}=\int_V \boldsymbol{S}^T\boldsymbol{f}\left|\boldsymbol{D}\right|dV\ \ or\ \ \boldsymbol{Q}_e=\boldsymbol{S}^T\boldsymbol{F}\left|\boldsymbol{D}\right|$$

where $\boldsymbol{f}$ is volume force and $\boldsymbol{F}$ is concentrated force.

The structure dynamics differential algebraic equations (DAEs) is

$$\begin{bmatrix}\boldsymbol{J}_1 & \boldsymbol{C}_q^T\\ \boldsymbol{C}_q & 0\end{bmatrix}\cdot\begin{bmatrix}\Delta\boldsymbol{q}\\ \Delta\boldsymbol{\lambda}\end{bmatrix}=\begin{bmatrix}\boldsymbol{F}_1\\ \boldsymbol{F}_2\end{bmatrix}$$

$$\boldsymbol{F}_1=\boldsymbol{M}\ddot{\boldsymbol{q}}+\boldsymbol{Q}_k-\boldsymbol{Q}_e\quad \boldsymbol{J}_1=\partial\mathbf{F}_1/\partial\boldsymbol{q}\quad \boldsymbol{C}_q=\partial\boldsymbol{C}/\partial\boldsymbol{q}$$

where $\boldsymbol{q}$ is system generalized coordinates, $\boldsymbol{F}_1$ is Jacobi matrix of dynamics equations, $\boldsymbol{C}$ is constraint equations. As $\boldsymbol{J}_1$ matrix is asymmetric band sparse matrix, a reshaping technique (Fig.5) is applied and Guass-Seidel iteration is used to solve linear equations. If the bandwidth $m$ is much smaller than matrix dimension $n$, the computation cost reduce to $O(m^2/n^2)$ compared with direct elimination method.

## 3. Validation cases of ANCF plate and shell element

### 3.1 Inflation of a square airbag

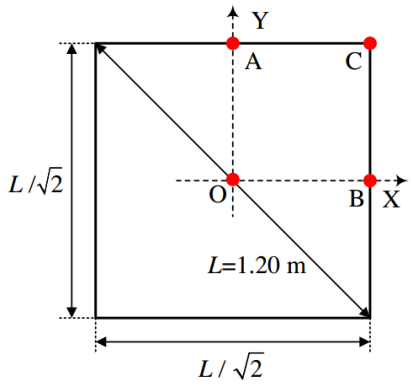


**Figure 6.** Initial configuration of square airbag

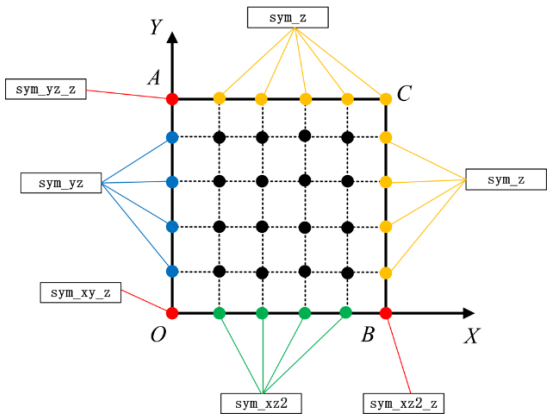


**Figure 7.** Symmetric boundary condition of for ANCF element nodes

As shown in Fig.6, an initial square flat membrane is placed in the horizontal plane and subjected to an internal pressure $p$=5000Pa. The length $L$ of the diagonal line of the airbag and the thickness of the membrane are 1.2m and 0.06mm respectively. The Young's modulus and Poisson's ratio are 588MPa and 0.4 respectively. Point O is the middle point while A and B are the middle points of two edges. The symmetric condition enables one to study only one quarter (OBCA) of the upper airbag.

OBCA is discretized by 10×10 ANCF elements, 6 types of boundary conditions and constraint equations of ANCF nodes is applied as in Fig. 7. Fig. 8 shows the 1/4 airbag inflation configuration and von Mises contour, which agrees well with the results of Liu [18]. The displacement relative error of O, B and C are 2.91%, 2.26% and 5.87%.

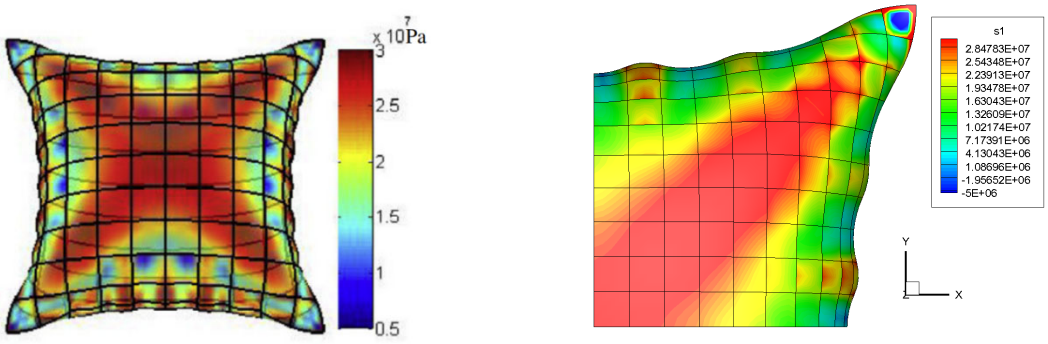


**Figure 8.** Airbag inflation configuration and von Mises contour by Liu [18] (left) and current result (right)

### 3.2 Hemispherical shell with 18° hole

The test case is a classical double-curved shell problem commonly used to assess the element's ability to reproduce a correct membrane and bending state. The initial configuration is one quarter of a hemispherical shell with 18° hole at the top. The sphere radius is 10m with thickness 0.04m. The Young's modulus and Poisson's ratio are $6.825\times10^7$Pa and 0.3. Two concentrated force is applied at point A and B respectively as each force is P/2 (Fig. 9).

The one quarter hemisphere is discretized with 15×12 elements. Fig. 10 exhibits the deformation by Yan [17] and current results. The maximum Y displacement is 8.5m with relative error 4.9%.

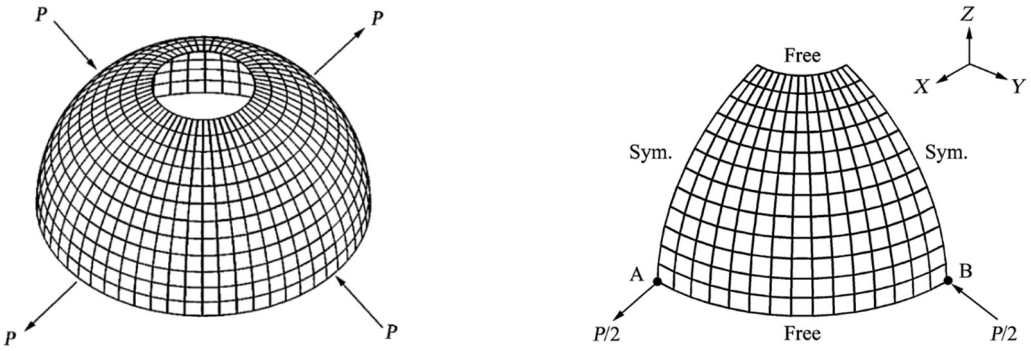


**Figure 9.** Hemisphere shell with 18° hole (left) and one quarter model with boundary condition (right)

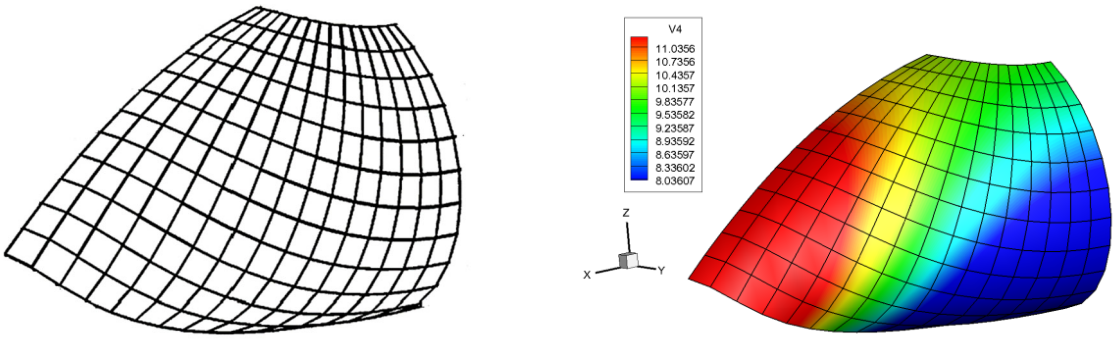


**Figure 10.** Hemispherical shell deformation by Yan [17] (left) and deformation by ANCF shell element (right)

## 4. C-9 parachute inflation configuration with ANCF shell element

C-9 parachute is a classic circle flat parachute model. The geometry and material parameters are shown in **Table 1**. The inflow velocity is V=80m/s and air density $\rho$=1.18kg/m$^3$. Assume that the canopy drag coefficient is $C_d$=0.5, the aerodynamic load on canopy can be given as P=0.5$\rho C_d V^2$=1824Pa.

Considering the symmetric condition, only a quarter of C-9 canopy is modeled and simulated. The 1/4 canopy is discretized into 7 ANCF thin shells, each shell has 2×6 ANCF shell elements. The total elements is 84, which is only 1/10 scale of classic FEM mesh.

**Table 1.** C-9 parachute geometry and material parameters

| | |
|---|---|
| Diameter of main canopy | 8.5m |
| Number of radial member | 28 |
| Length of suspension line | 9m |
| Diameter of canopy hole | 0.85m |
| Canopy material density | 533.77kg/m$^3$ |
| Canopy material Young's modulus | 0.4309GPa |
| Canopy material Poisson's ratio | 0.14 |
| Thickness of canopy | 0.0001m |
| Density of suspension line material | 462kg/m$^3$ |
| Young's modulus of suspension line | 97GPa |

The uniform distributed pressure on each element is

$$\boldsymbol{Q}_e = abp\int_0^1\int_0^1 \boldsymbol{S}^T \boldsymbol{n}_Z |\boldsymbol{D}| d\xi d\eta$$

where $a$, $b$ and $p$ are the material length, width and thickness of shell plates, $\boldsymbol{n}_z$ is the normal vector of local position.

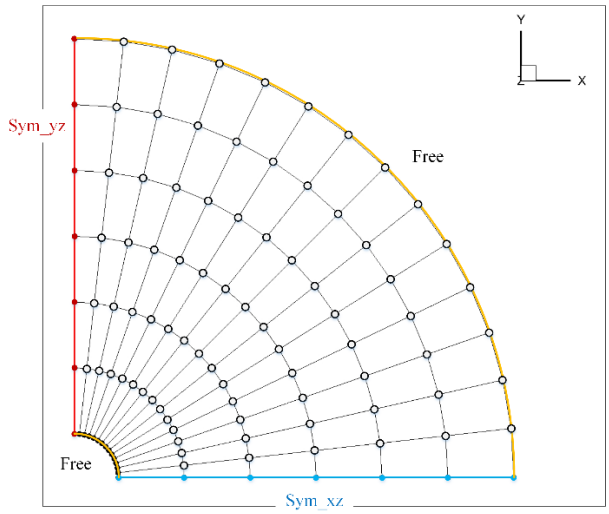


**Figure 11.** Discretization of 1/4 C-9 canopy initial inflation configuration

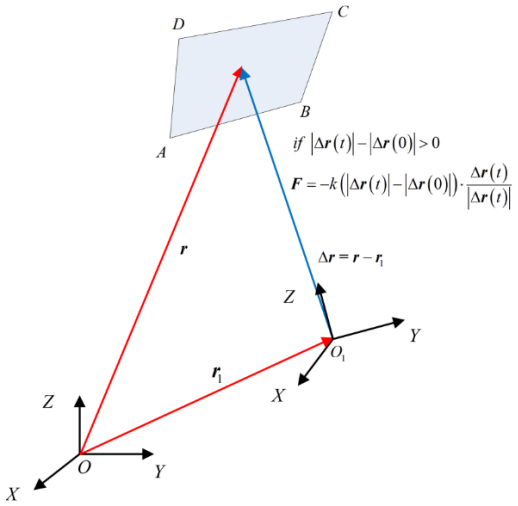


**Figure 12.** Spring force between arbitrary point r in shell element ABCD and fix point $O_1$

The boundary conditions is shown in Fig.11. At each common node between adjacent shells, shell node sphere constraint equations are applied. The suspension lines are modeled as a series of spring force as in Fig.12, in which the spring stiffness $k=E \cdot S/L$=5.29189e4 N/m. The tensile force $\boldsymbol{F}$ is

$$\boldsymbol{F} = -k\left(|\Delta\boldsymbol{r}(t)| - |\Delta\boldsymbol{r}(0)|\right)\cdot\Delta\boldsymbol{r}(t)/|\Delta\boldsymbol{r}(t)| \quad if\ |\Delta\boldsymbol{r}(t)| - |\Delta\boldsymbol{r}(0)| > 0$$

By applying band sparse matrix reshaping technique, the computation cost is greatly saved and a single-process calculation is used for C-9 inflation process simulation in t=1.0s Fig. 13 shows the converged 1/4 C-9 inflation configuration and von Mises stress contour, which highlight the region of high stress and provide structure strengthening and optimization for such parachutes.

## 5. Conclusion

A generic shell element based on absolute nodal coordinate formulation (ANCF) is developed to model parachute canopy to reduce computation resources and retain membrane strain/stress analyzing capability. Multiple validation cases of ANCF plates and shell elements have been conducted and compared with the current literature, where large deformation configurations and stress distribution have been verified. A 1/4 C-9 parachute canopy inflation process with uniform pressure is simulated with the 1/10 mesh scale of classical FEM at a much reduced computational cost.

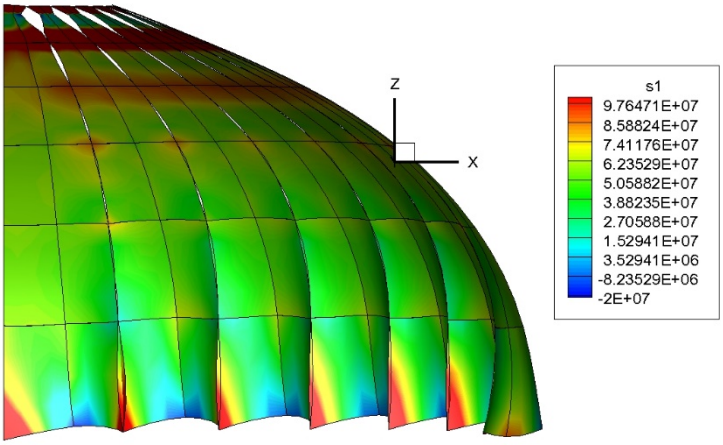


**Figure 13.** The converged 1/4 C-9 inflation configuration and von Mises stress contour

## Acknowledgment

This paper is supported by the National Science Foundation of China (Grant No. 12102446).

## References

[1] Zhenlong Xu, Michael Accorsi, John Leonard. Simulation of dynamic contact problems in parachute systems [J]. Journal of Aerospace Computing, Information, and Communication. 2004. Vol.1: 288-307.

[2] Kenji Takizawa, Samuel Wright, Creighton Moorman, Tayfun E. Tezduyar. Fluid–structure interaction modeling of parachute clusters [J]. International Journal for Numerical Methods in Fluids, 2011,65: 286-307.

[3] Purvis J. W. Theoretical analysis of parachute inflation including fluid kinetics [J]. AIAA, 1981, 1925: 336-342.

[4] Purvis J. W. Numerical prediction of deployment, initial fill, and inflation of parachute canopies [J]. AIAA, 1984, 84 (0787)

[5] Masaya MIYOSHI, Takuya ISHII, etc. Computational Analysis of Parachute Motions Using the Immersed Boundary Method [C]. 46th AIAA Aerospace Sciences Meeting and Exhibit, 7 - 10 January 2008, Reno, Nevada

[6] Joung-Dong Kim Yan Li, Xiaolin Li. Simulation of parachute FSI using the front tracking method [J]. Journal of Fluids and Structures, 2013, 37: 100-119

[7] Qiangqiang Shi, Daniel Reasor, Zheng Gao, Xiaolin Li, Richard D. Charles. On the verification and validation of a spring fabric for modeling parachute inflation [J]. Journal of Fluids and Structures, 2015(58): 20-39.

[8] Keith R.Stein Richard J. Benney. Parallel computation of parachute fluid-structure interactions [A]. In.AIAA Aerodynamic Decelerator Systems Technology Conference, 14th, [C]. San Francisco,CA: AIAA, 1997

[9] Keith Stein, Richard Benney, Tayfun Tezduyar, at al. Fluid-structure interaction simulation of a cross parachute: comparison of numerical predictions with wind tunnel data. [J]. AIAA-99-1725: 172-181

[10] K. Karagiozis R. Kamakotic, F. Cirak, C. Pantano. A computational study of supersonic disk-gap-band parachutes using Large-Eddy Simulation coupled to a structural membrane [J]. Journal of Fluids and Structures, 2011, 27: 175-192

[11] A. Shabana A. Definition of the slopes and the finite element absolute nodal coordinate formulation [J]. Multibody System Dynamics, 1997, 1(3): 339-348

[12] Wan-Suk Yoo Oleg Dmitrochenko, Dmitry Yu. Pogorelov. Review of finite elements using absolute nodal coordinates for large-deformation problems and matching physical experiments [A]. In.ASME 2005 International Design Engineering Technical Conferences & Computers and Information in Engineering Conference [C]. Long Beach,California,USA, 2005.

[13] Johannes Gerstmayr Hiroyuki Sugiyama, Aki Mikkola. Review on the absolute nodal coordinate formulation for large deformation analysis of multibody systems [J]. Journal of Computational and Nonlinear Dynamics, 2013, 8(031016): 1-12.

[14] K.Dufva Shabana, A. A. . Analysis of thin plate structures using the absolute nodal coordinate formulation [J]. Proc.Inst.Mech.Eng.,Part K: J.Multi-body Dyn., 2005, 219(4): 345-355

[15] Mikkola A.M., Shabana.A.A. A Non-Incremental Finite Element Procedure for the Analysis of Large Deformation of Plates and Shells in Mechanical System Applications [J]. Multibody Syst. Dyn., 2003, 9: 283-309

[16] O. N. Dmitrochenko D. Yu. Pogorelov. Generalization of plate finite elements for absolute nodal coordinate formulation [J]. Multibody Syst. Dyn., 2003, 10: 17-43

[17] D. Yan. C.Liu., Q.Tian.,K.Zhang.,X.N.Liu. A new curved gradient deficient shell element of absolute nodal coordinate formulation for modeling thin shell structures [J]. Nonlinear Dyn, 2013, 74: 153-164

[18] Cheng Liu, Qiang Tian, Dong Yan, Haiyan Hu. Dynamic analysis of membrane systems undergoing overall motions, large deformations and wrinkles via thin shell elements of ANCF, Comput. Methods Appl. Mech.Engrg. 2013(258):81-95.